MICROSOMAL T SYSTEM

A Stereological Analysis of Purified Microsomes Derived from Normal and Dystrophic Skeletal Muscle

DONALD J. SCALES and ROGER A. SABBADINI

From the Laboratory of Physiology and Biophysics, University of the Pacific, San Francisco, California 94115; and the Department of Biology and Molecular Biology Group, San Diego State University, San Diego, California 92182

ABSTRACT

Heterogeneous populations of microsomes obtained from normal and dystrophic chicken pectoralis muscle were separated into two subfractions by an iterative loading technique. The buoyant density of the sarcoplasmic reticulum (SR) microsomes was increased after loading them with calcium oxalate. Several incubations in the transport medium were necessary to load all of the SR. The fraction that did not form a pellet contained microsomes which displayed freeze-fracture faces that had a low density of particles. A stereological analysis was used on membrane fracture faces of intact muscle to generate reference particle density distributions, which were compared with the distributions measured on the microsomal fracture faces. The concave microsomal fracture faces of purified microsomes which did not load calcium oxalate had particle distributions nearly identical to the distributions of intact P-face T tubules. The morphological data suggest that this subfraction is microsomal T system. Biochemical measurements show negligible amounts of specific Na^+, K^+-ATPase activity, suggesting that there was little contamination from the surface membrane in this subfraction. Furthermore, an active Ca^{2+}-ATPase is demonstrated in both normal and dystrophic T-tubular membranes.

KEY WORDS   transverse tubules · freeze-fracture stereology · muscular dystrophy · microsomal subfraction · skeletal muscle

This paper describes a procedure for isolating membrane fragments of the transverse tubular system of skeletal muscle. Because the only definitive markers for transverse tubules are their structural characteristics, we developed a purification scheme based on morphological measurements. Once these membranes were identified and shown to originate from the T tubules, we measured the protein composition and began a general biochemical analysis which we will present in another publication.

It is apparent from the prolific freeze-fracturing data which has appeared in the literature over the past few years that membranes display freeze-fracturing characteristics unique to their function. That is, each membrane displays a unique freeze-fracture "signature," which is most conveniently expressed as a distribution of particle densities. This profile can be used to identify a membrane after freeze fracture and is the basis for the recent

stereological analysis suggested by Weibel et al. (23) and used by Losa et al. (15) to analyze microsomal subfractions from liver. Microsomal membrane classes are identified on the basis of particle density profiles of membranes observed in intact cells of tissue from which the microsomes are derived. The underlying assumption of this method is that the particle density profiles remain invariant during homogenization and centrifugation. In this paper, we use Weibel's stereological method to identify a purified microsomal subfraction consisting of low particle density fracture faces derived from skeletal muscle.

Early attempts to isolate microsomal subfractions from normal and dystrophic chicken pectoralis muscle showed no structural differences between the two fractions (2). However, normal and dystrophic muscle microsomes isolated in our laboratory revealed several morphological differences, including a reduction in mean particle density for dystrophic vesicles. Moreover, heterogeneous populations of vesicles were obtained where most of the dystrophic concave freeze-fracture faces demonstrated few or no particles and most of the normal concave faces showed a high density of particles characteristic of sarcoplasmic reticulum (SR) membranes (17). It was suggested by Malouf and Sommer (16) that the proliferation of low particle density microsomes observed in our dystrophic preparation could originate from expanded T-tubular elements which they observed in older animals (8–18 mo) with avian muscular dystrophy. We subsequently confirmed Malouf and Sommer's observation by showing that a similar proliferation of T tubules was present in thin-sectioned and freeze-fractured whole muscle tissue of 5–6-wk-old animals, which were free of the atrophic alterations characteristic of older animals (19).

Dystrophic microsomal fractions isolated from these younger animals contained nearly twice the relative amount of low particle density concave fracture faces as the normal. We then subjected these mixed preparations to discontinuous sucrose gradient centrifugation in an attempt to separate the light vesicles (presumably T tubules) from the high particle density SR on the basis of different buoyant densities. However, complete separation of the SR from T-tubular membranes was not obtained.

In this paper, we describe a more effective procedure for separating the low particle density microsomes from the SR and, on the basis of a

stereological analysis of freeze-fracture replicas, we identify this purified subfraction as microsomal T system. In other experiments, we compare the morphological and biochemical characteristics of normal T-tubular vesicles to those of T-tubular vesicles derived from dystrophic muscle.

MATERIALS AND METHODS

Preparation of Mixed Microsomes

Normal (line 412) and dystrophic (line 413) New Hampshire chickens were obtained from the Department of Avian Sciences, University of California, Davis and sacrificed at 5–8 wks of age. Microsomes were prepared from the pectoralis major by the method of Inesi (see Scales et al. [19]). When applied to chicken muscle, this procedure results in the so-called "mixed microsomal" preparation consisting of a heterogeneous population of vesicles from all elements of the sarcotubular system.

Separation of a Light Fraction

The separation of a light fraction from SR microsomes in the mixed preparation was performed according to the method of Sabbadini et al. (18). The mixed microsomal preparation was incubated for 10 min at 37°C in a reaction mixture containing 20 mM morpholinopropane sulfonic acid (MOPS) (pH 6.8), 2 mM $CaCl_2$, 2 mM EGTA, 5 mM ATP, 80 mM KCl, 5 mM K-oxalate, and 0.3 mg microsomal protein/ml. A 30-ml aliquot was layered on a 4-ml cushion of 52% sucrose, 20 mM MOPS at 5°C. The suspension was centrifuged for 45 min at 82,500 g in a Beckman L5-50 Ultracentrifuge equipped with a SW 27 rotor (Beckman Instruments, Inc., Spinco Div., Palo Alto, Calif.).

After centrifugation the fraction that did not enter the sucrose was removed, incubated a second time in fresh reaction mixture, and centrifuged again. This was repeated until no pellet was formed. For the dystrophic microsomes this occurred after the third spin, but a third pellet was formed in the normal case. The third (normal) supernate was incubated again at 37°C for 10 min in fresh reaction mixture, cooled to 5°C, and layered on a discontinuous sucrose gradient consisting of 4 ml of 52% sucrose, 20 mM MOPS, and 4 ml of 28% sucrose buffer. After centrifugation the fraction sedimenting above the 28% sucrose was withdrawn and resuspended in 30% sucrose, 25 mM imidazole-HCl (pH 7.0). This procedure is summarized in Fig. 1.

Freeze Fracture

Samples of whole muscle pectoralis were fixed by immersion in 4% glutaraldehyde for 15 min in 0.1 M cacodylate (pH 7.2), rinsed, and gradually infiltrated with 20% glycerol. After 1-h, samples were frozen in liquid Freon 22, fractured, and replicated on a Balzers 360 M (Balzers Corp., Nashua, N. H.) at −100°C, 2 × 10^{-6} Torr.

ISOLATION PROCEDURE

FIGURE 1 The technique used to separate the mixed microsomal preparations into two distinct subfractions. The SIII fraction of the dystrophic microsomes and the SIV fraction of the normal microsomes were analyzed by freeze-fracture stereology.

The microsomes were washed free of sucrose and 25 mM imidazole-HCl, and resuspended in 0.2 ml of 60 mM KCL, 10 mM MOPS, and 20% glycerol. After 2 h, drops of the sample were frozen in liquid Freon 22, fractured, and replicated on a Balzers 360 M at $-100°C$, 2×10^{-6} Torr. All platinum carbon replicas were examined in a Philips EM200 at 80 kV.

Stereological Procedure

The electron-optical magnification was calibrated with a diffraction grating, and the negatives were enlarged 10 times optically to a final print magnification of 147,000. A test circle of area A was applied to the fracture faces to generate the particle density distribution in each case. This sampling area determines the resolution of the distribution. One must select a particle density interval, $\Delta\rho$, for the histogram (also referred to as the "bin size" by stereologists) so that there are no gaps in the final distribution caused by the sampling. If the change in the number of particles that we wish to detect is Δn, then the bin size must be

$$\Delta\rho \gtrsim \frac{\Delta n}{A}.$$

At best, we want $\Delta n = 1$ particle, then

$$\Delta\rho \gtrsim \frac{1}{A} \text{ particles/}\mu m^2.$$

In our case, a 12-mm circle corresponds to a test area of $5.23 \times 10^{-3} \mu m^2$, so that

$$\Delta\rho \gtrsim 190 \text{ particles/}\mu m^2.$$

A 12-mm test circle, then, generates a particle density distribution with a bin size that we choose, for convenience, to be 200 particles/μm^2.

The test circle was centered on microsomal concave fracture faces that had no cast shadow, and the number of particles enclosed by the circle was counted. Particles

that intersected the test circle were counted alternately in and out. A total of 109 normal concave faces and 65 dystrophic faces were counted.

Intact sarcolemma (SL) and T tubules were measured with the same 12-mm circle placed randomly on P fracture faces of these membranes also magnified to × 147,000. 50-200 test circle applications were used to generate these reference particle density profiles.

ATPase Activity Measurements

ATP hydrolysis rates of isolated membranes were determined by using a coupled assay system which followed the oxidation of NADH as ADP was formed by the ATPase enzyme. The basic reaction mixture contained 50 mM imidazole-HCl (pH 7.0), 5 mM MgCl₂, 1 mM EGTA 3 mM phosphoenopyruvate, 25 U/ml pyruvate kinase, 40 U/ml lactate dehydrogenase, 0.2 mg/ml NADH, and 25-50 μg protein/ml. Reactions were carried out at 37°C immediately following the isolation of microsomal protein. The reaction was initiated by the addition of 1 mM ATP (Calbiochem-Behring Corp., American Hoechst Corp., San Diego, Calif.), and a basal level of Mg^{2+}-ATPase activity was obtained for the enzyme. Linear rates of calcium-activated Mg^{2+}-ATPase were obtained by adding to the cuvette 100 μM X537A (in 1-propanol) followed by 1 mM CaCl₂.

In experiments designed to purify the Na^+, K^+-ATPase enzyme, T-tubular membranes were treated with deoxycholate according to the procedures of Jorgensen and Skou (10). T-tubular protein (0.25 mg) was treated with 0.06% deoxycholate and 2 mM EGTA for 30 min at 23°C. The membranes were centrifuged for 30 min at 25,000 g. The pelleted membranes were resuspended in 30% sucrose, 25 mM imidazole-HCl (pH 7.0).

RESULTS

Whole Muscle Fracture Faces

Freeze-fracture replicas of normal and dystrophic sarcotubular membrane systems are shown in Fig. 2. The normal T tubule is compact and highly curved, and is flanked by the neighboring cisternae of the junctional SR joined by regularly spaced junctional processes. The dystrophic T system is enlarged as described earlier (19), and this affords more expansive views of the membrane. In both cases, the T tubule has a low particle density on both P and E faces and is flanked by junctional SR which has a much higher P-face particle density and nearly smooth E face.

P faces of T tubules were identified as troughlike concave fracture faces oriented perpendicular to the fiber axis and in the proximity of the high particle density concave fracture faces of the adjacent junctional SR. Longitudinal fracture planes
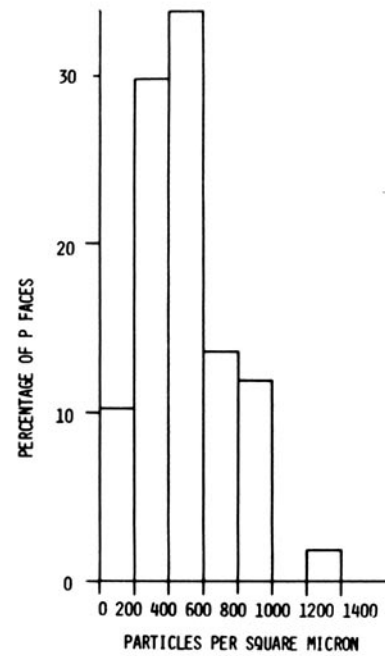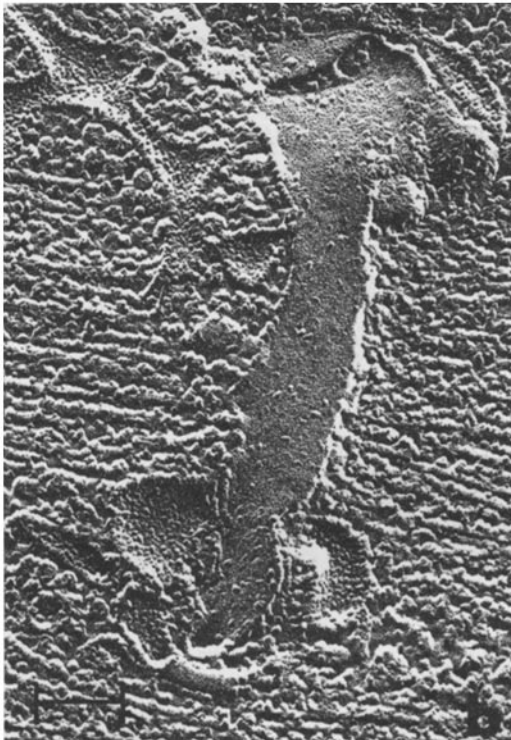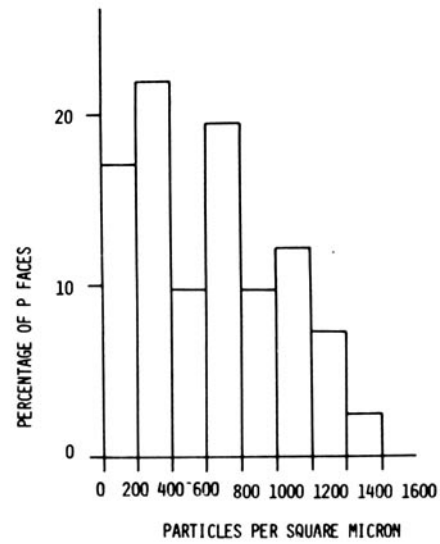
FIGURE 2 (a) Freeze-fracture replica of the normal sarcotubular system. The cisternae of the junctional SR flank both sides of the slender T tubule. This fracture shows the P face of the nonjunctional T system. The histogram to the right shows the particle density distribution of P fracture faces combined from both junctional and nonjunctional T system. The technique for measuring these densities is explained in Materials and Methods. × 94,100. (b) Freeze-fracture replica and P-face particle density profile of the dystrophic sarcotubular system. The enlarged membranes of the T system afford views of more expansive fracture faces. Elements of the junctional SR (high particle density) are visible on both sides of the T tubule at the bottom of the micrograph, and a fragment of free SR is seen at the top left. The particle density profile is distinctly different from that of the normal T system and has an overall lower mean density (see Table I). Bars, 0.1 μm (for all figures). × 94,100.
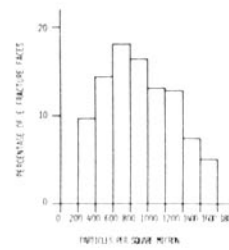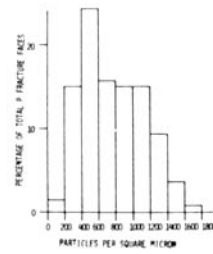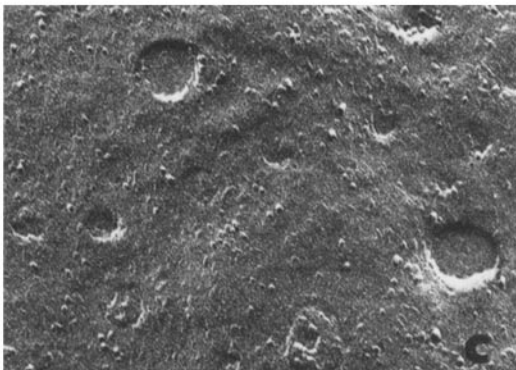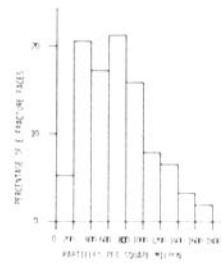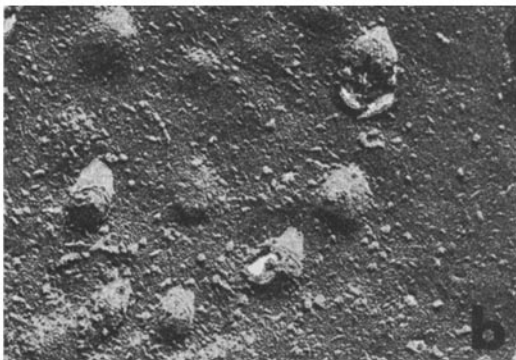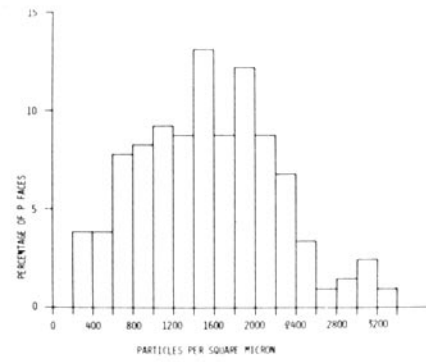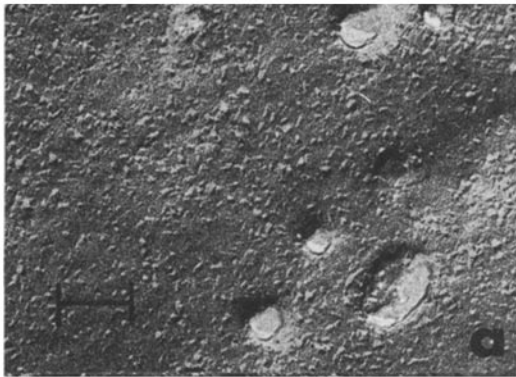
FIGURE 3   (a) Normal SL: P face. × 94,100. (b) Normal SL: E face. × 94,100. (c) Dystrophic SL: P face. × 94,100. (d) Dystrophic SL: E face. × 94,100.

of this type revealed the nonjunctional aspect of the T tubules. This is the most highly curved part of the tubule, and measurements of the particle density are hindered by the frequently obscurant cast shadow. Fractures transverse to the fiber axis revealed the junctional aspect of the T system. This produced more shallow fracture faces, which were more amenable to the sampling technique. Fracture faces of both types were used to generate the particle density profiles as described in Materials and Methods and shown in Fig. 2 a for normal and Fig. 2 b for dystrophic muscle. Mean values of the P-face particle densities are $690 \pm 60/\mu m^2$ for the normal T tubule and $560 \pm 30/\mu m^2$ for the dystrophic one.

The surface membrane displays fracture faces distinctly different from those of the T tubules. The most notable difference arises from the presence of caveolae which form large depressions on the sarcolemmal P fracture faces and protuberances on the E faces. Fig. 3 a–d shows both leaflets of the normal and dystrophic SL as well as their particle density profiles. Table I summarizes the mean particle densities measured from these fracture faces. Contrary to most other plasma membranes, the dystrophic SL displays a higher particle density on its extracellular leaflet, and furthermore, this density is higher than that of the normal sarcolemmal E face. The dystrophic P face shows a reduced density of particles compared with the normal P face.

Mixed Microsomal Preparation

Figs. 4 and 5 show micrographs of the standard subfractions, the so-called "mixed microsomal" preparations of normal and dystrophic muscle. The accompanying particle density profiles of the concave fracture faces for these microsomes show that both distributions are trimodal, but the relative number of microsomes in each group is dif-

ferent. 38% of the dystrophic microsomes have a particle density $<2,000/\mu m^2$, whereas these low particle density microsomes account for only 20% of the normal preparation. It is these low particle density microsomes that we attempt to isolate by the iterative loading technique. The ranges of particle densities for the T system, SL, and junctional and longitudinal SR obtained from whole muscle freeze-fracture replicas are indicated above.

Purified Microsomes

In contrast to chicken breast microsomes, those obtained from rabbit leg and lobster tail consist of a homogeneous population of vesicles derived from the SR with <5% contamination from other sources. We would expect all of the SR vesicles to load calcium oxalate and enter a sucrose cushion; however, other investigators have succeeded in getting only 30–50% of the initial SR protein to appear in a pellet after loading with calcium oxalate (3, 8). We have found that it is possible to ultimately pellet 95% of rabbit SR protein if the unloaded vesicles which initially do not enter the sucrose layer are repeatedly incubated in fresh transport medium and centrifuged again.

The mixed microsomal preparation from the chicken was subjected to this iterative loading and centrifugation scheme, as outlined schematically in Fig. 1, to separate vesicles that accumulated calcium from those that accumulated little or no calcium. We repeated the loading procedure until no pellet was formed, at which time all active SR should be removed. This occurred after the third spin for the dystrophic microsomes. We found that it was necessary to add an additional step to purify the normal microsomes and to do a fourth spin in a discontinuous sucrose gradient to remove any inactive SR vesicles that might not have loaded calcium oxalate. Representative freeze-fracture

TABLE I

Mean Particle Densities

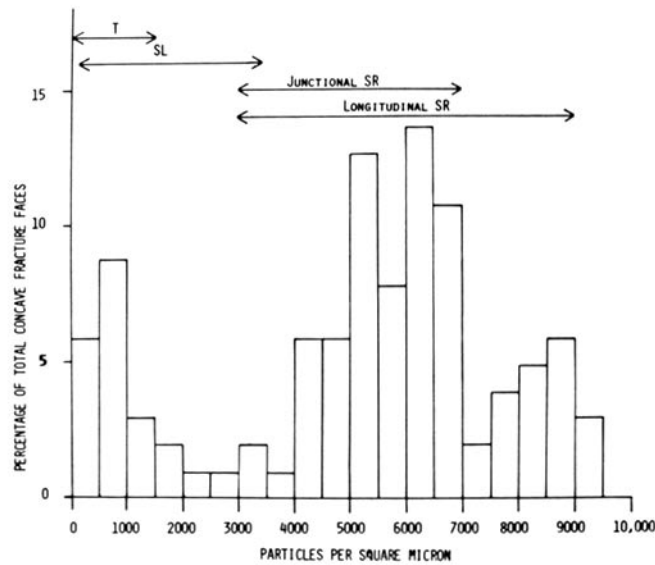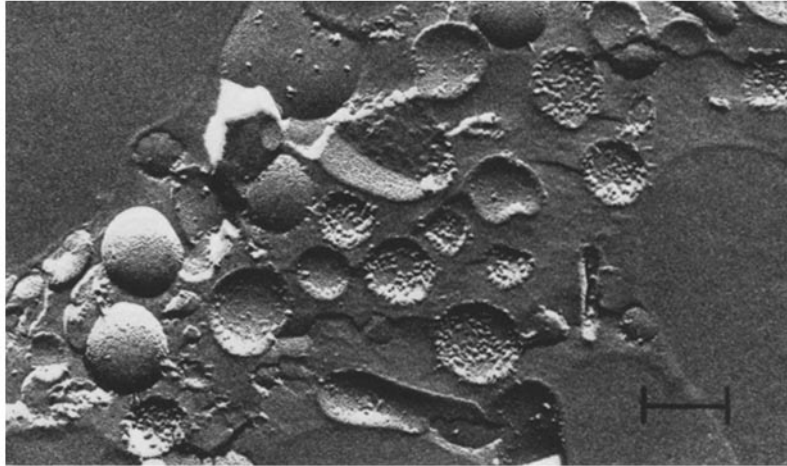| Fracture face	Normal	Dystrophic
	particles/μm^2	
SL, P face	$1,630 \pm 50$ (207)	750 ± 30 (140)
SL, E face	790 ± 30 (151)	900 ± 30 (289)
T tubule, P face	690 ± 60 (41)	560 ± 30 (59)
Microsomes, concave face	680 ± 40 (109)	480 ± 30 (65)
convex face	540 ± 50 (85)	510 ± 30 (118)

Sample size is given in parentheses.

FIGURE 4   An overview of microsomes derived from the normal pectoralis muscle, the so-called "mixed microsomal" preparation. The heterogeneous population of fracture faces is reflected in the accompanying histogram which shows that concave fracture faces are present with a wide variety of particle densities. The ranges indicated at the top were observed on freeze-fracture replicas of intact muscle and show the limits of the T system, sarcolemma (SL), and SR. × 102,000.

micrographs of these subfractions are shown in Fig. 6 for normal and Fig. 7 for dystrophic microsomes. All of the microsomes exhibit a sharp boundary and a low particle density on both fracture faces. None of the concave fracture faces examined had particle densities above $1,600/\mu m^2$ (normal or dystrophic). The concave particle density profiles of the purified microsomes are also shown in Figs. 6 and 7. The average particle densities are $680 \pm 40/\mu m^2$ for normal microsomes

and $480 \pm 30/\mu m^2$ for dystrophic microsomes (Table I). Although some of the microsomes were elongated and resembled tubular shapes, most of the vesicles produced round profiles from spherical vesicles.

ATPase Activities

The nonspecific (Mg^{2+}-activated) and Na^+, K^+-activated Mg^{2+}-ATPase activities of purified T-tubular fractions of normal and dystrophic muscle
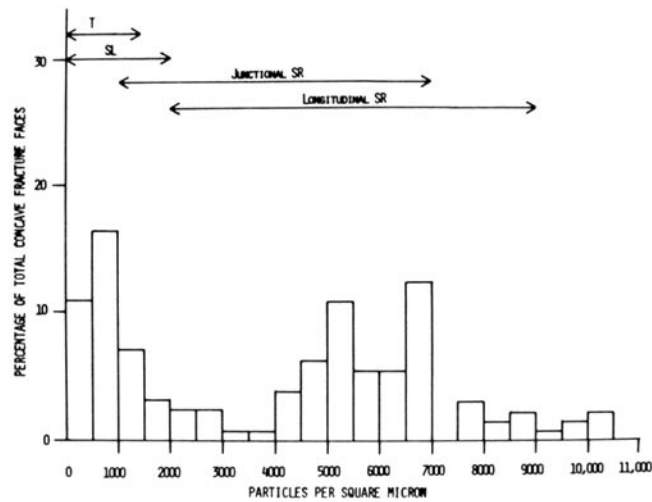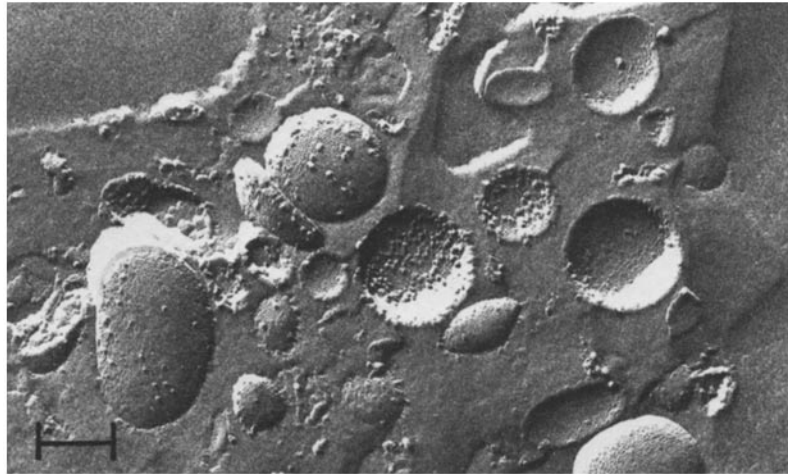
FIGURE 5 The mixed microsomal preparation from dystrophic pectoralis. The relative amount of low particle density concave fracture faces is much greater than the normal preparation (note different vertical scale). We separate the low density microsomes by increasing the buoyant density of the SR microsomes by actively loading them with calcium oxalate and then centrifuging. × 102,000.

are shown in Table II. T-tubular membranes of both normal and dystrophic muscle contained negligible amounts of specific Na^+, K^+-ATPase activity even after deoxycholate treatment. The average Na^+, K^+-ATPase activity produced by native (nondetergent treated) normal membranes was 3.2 μmol/mg protein/h. This value is severalfold lower than that commonly observed for highly purified fractions of sarcolemmal membranes (11). Moreover, the absence of sarcolemmal contamination is also suggested by our inability to purify the Na^+, K^+-ATPase after detergent treatment. In experiments in which Triton X-100 (0.005–0.1%)

was added to the incubation mixture before ATPase determinations, we could not observe any stimulation of ATPase activity by sodium and potassium (data not shown). This indicates that the lack of availability of substrates to the inside of the vesicles was not responsible for the low levels of Na^+, K^+-ATPase observed for the native membrane.

On the other hand, high levels of specific Ca^{2+}-ATPase activity were obtained for both normal and dystrophic T-tubular membranes isolated by the iterative loading technique (Table III). Specific Ca^{2+}-ATPase rates of 2.19 and 1.44 μm ADP/mg
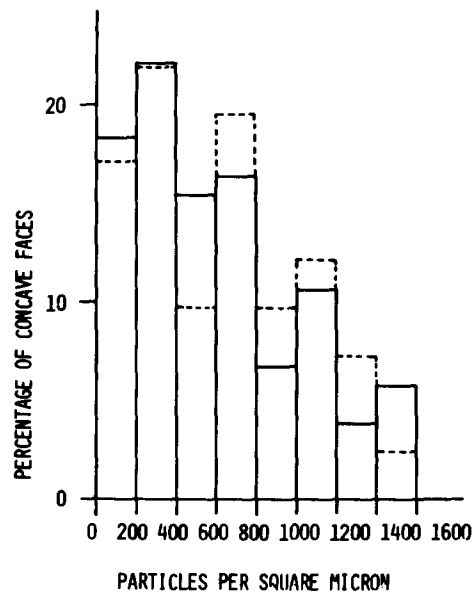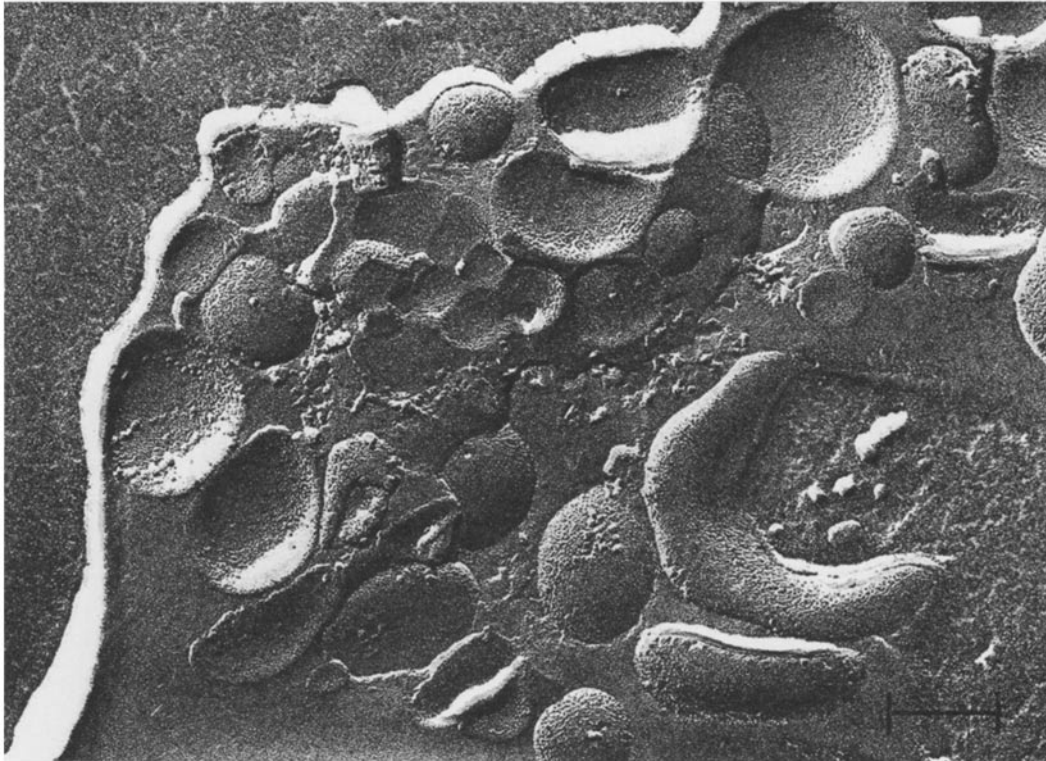
FIGURE 6 After repeated incubations of the normal mixed microsomes in transport medium, the subfraction that does not form a pellet or enter the 28% sucrose layer is shown here. The concave fracture face particle density profile is shown below by the solid lines. For comparison, the P-face profile of the intact T system from Fig. 2 a is indicated by dashed lines. The similarity of the two profiles indicates that we have isolated microsomes from the T system. × 148,000.
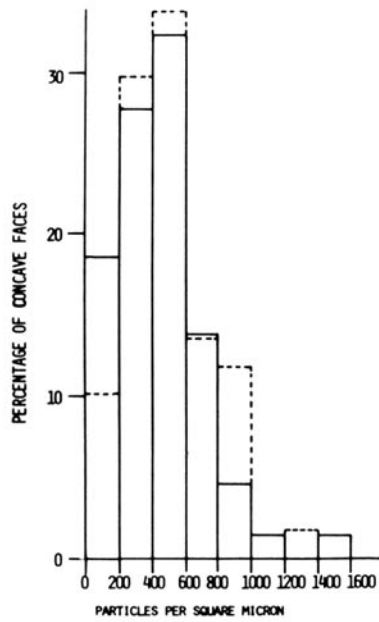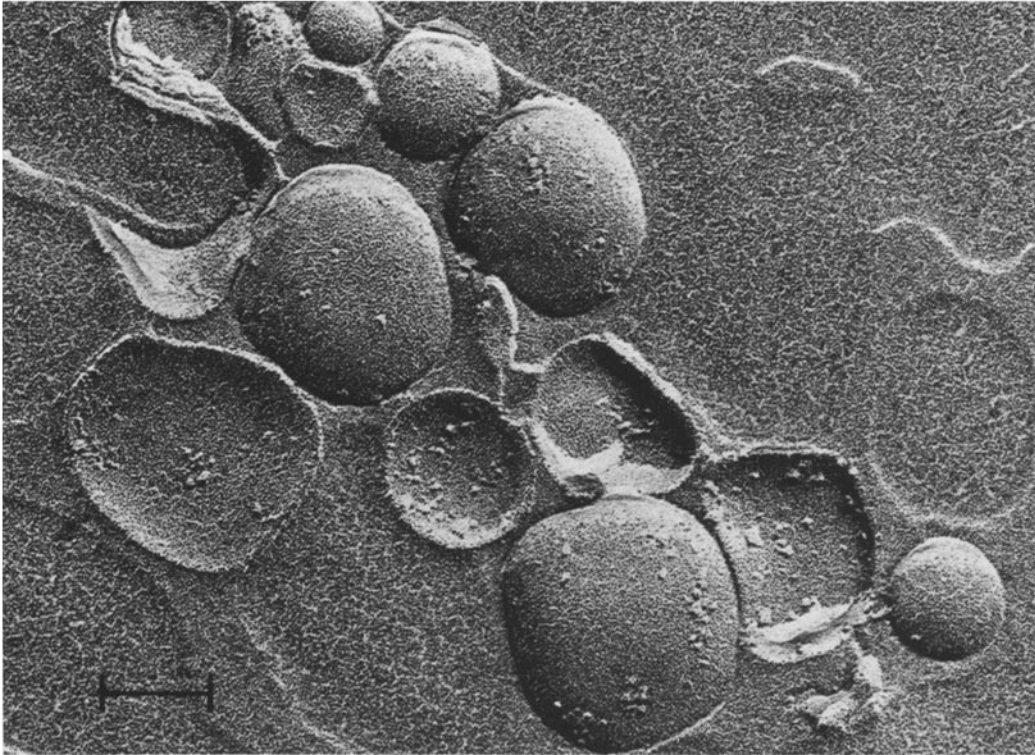
FIGURE 7 A freeze-fracture replica of the purified subfraction from the dystrophic mixed microsomes. The concave fracture-face particle density profile is shown below by the solid lines. The P-face profile of the intact dystrophic T system from Fig. 2 b is indicated by dashed lines. × 134,000.

TABLE II

Na^+,K^+,Mg^{2+}-ATPase Activities of Native and Detergent-Treated T-Tubular Membranes

	Mg^{2+}-ATPase*	Na^+,K^+,Mg^{2+}-ATPase
Normal		
100 mM NaCl	22.3 ± 2.98	25.5 ± 2.54
10 mM KCl		
(n = 4)		
DOC treated	21.9	20.5
100 mM NaCl		
10 mM KCl		
(n = 2)‡		
Dystrophic		
100 mM NaCl	26.0	27.25
10 mM KCl		
(n = 2)‡		
DOC treated	33.78 ± 3.0	36.95 ± 5.2
100 mM NaCl		
10 mM KCl		
(n = 4)		

* Values are μmol ADP released/mg protein/h ± 2 SEM at 37°C.

‡ Sample size not large enough for statistical analysis.

protein/min were observed for dystrophic and normal preparations, respectively. The Ca^{2+}-ATPase rates observed for dystrophic T-tubular membranes were significantly higher than those observed for the normal membrane.

It is interesting to note that the specific Ca^{2+}-ATPase activity of dystrophic mixed microsomal membranes (consisting primarily of SR protein) was not significantly different from those of the normal when measured under these conditions (i.e., in the presence of the ionophore X537A). The equivalence of normal and dystrophic Ca^{2+}-ATPase activities under conditions where no Ca^{2+} gradient is formed (i.e. with oxalate or detergents) has been reported previously (17, 19, 24).

DISCUSSION

Stereological and Biochemical Evidence for the Identification of T-Tubular Microsomes

Examination of whole muscle freeze-fracture replicas provides guidelines for the identification of membranes observed in isolated subfractions. The distribution of particles observed on the fracture face leaflets of the sarcotubular membrane system and the surface membrane are measured and used as references to establish the identity of muscle microsomes. The particle distributions of the fracture faces for T tubules and SL measured by applying a test circle are shown in Figs. 2 and 3 for normal and dystrophic skeletal muscle. The distributions for the normal and dystrophic T tubules agree qualitatively with similar measurements obtained with planimetry by Crowe and Baskin (7).

The mixed microsomal preparations contain an assortment of membrane fracture faces with maximum densities of $9,500/\mu m^2$ for normal and $10,500/\mu m^2$ for dystrophic fractions (Figs. 4 and 5). The method used for isolating these microsomes yields extremely pure preparations of SR from rabbit leg muscle (<5% contaminating membranes). In the chicken (both normal and dystrophic) a much more heterogeneous population of vesicles is obtained. Early attempts with the use of discontinuous sucrose gradients to produce homogeneous fractions of SR from these mixed microsomes did not eliminate the unidentified low particle density microsomes (19).

In the present paper, an iterative active loading technique is used to increase the buoyant density of the SR vesicles to separate them from the low particle density microsomes. Negative staining of the pelleted material demonstrated vesicles having the typical morphology of SR, i.e., 40-Å projections on the outer surface (unpublished observation). The interior of these vesicles contained highly unstable (in the electron beam) crystals of calcium oxalate, confirming that these microsomes had transported calcium. Freeze-fracture replicas showed that these vesicles had a high particle density on the concave face and none on the convex face, the freeze-fracture signature of SR. Furthermore, gel electrophoresis of these pellets demonstrated the characteristic protein pattern of SR, a major 106,000-dalton protein and two minor bands at 65,000 and 55,000 daltons. Our purification scheme, then, separated light microsomes from microsomes of SR.

Negatively stained images of the light microsomes, i.e., those that did not enter the sucrose layer, showed vesicles that were morphologically distinct from the pelleted SR. There were no surface projections or intravesicular calcium oxalate deposits. Because both SR and T-tubular vesicles possess calcium-dependent ATPase activities, it is curious that only SR vesicles are able to load calcium oxalate. Several explanations for the apparent inability of T-tubular vesicles to load calcium oxalate can be proposed: (a) T-tubular vesicles may be inside out and hence cannot establish

TABLE III

Ca^{2+},Mg^{2+}-ATPase Activities of the Mixed Microsomal And T-Tubular Fractions

	Mg^{2+}-ATPase*	Ca^{2+},Mg^{2+}-ATPase	Ca^{2+}-ATPase
Normal			
Mixed microsomes	0.3 ± 0.02	3.41 ± 0.3	3.1 ± 0.32
($n = 9$)			
T tubules	0.317 ± 0.1	1.72 ± 0.708	1.41 ± 0.64
($n = 10$)			
Dystrophic			
Mixed microsomes	0.43 ± 0.12	3.02 ± 0.52	2.60 ± 0.51
($n = 9$)			
T tubules	0.30 ± 0.06	2.50 ± 0.2	2.19 ± 0.22
($n = 10$)			

* Values are μmol ADP released/mg protein/min $\pm$ 2 SEM at 37°C.

intravesicular calcium concentration gradients, (b) the vesicles are right side in but cannot produce intravesicular concentrations of calcium necessary to exceed the solubility product for calcium oxalate, (c) T-tubular vesicles may be leaky to calcium, or (d) oxalate may not be permeable to the vesicles. Because rabbit T-tubular membranes isolated by the French press technique of Caswell (see Lau, et al. [14]) were shown to possess low oxalate permeability, it is likely that this is the explanation for the lack of calcium oxalate loading that we observe for chicken T-tubular vesicles, although further experimentation is required to eliminate the other possibilities.

The freeze-fracture particle density distributions of the concave fracture faces of these microsomes are shown in Figs. 6 and 7. For comparison, the profiles of the respective P faces from intact T tubules are shown as dashed lines. Despite a few small differences in peak heights, the general features of the microsomal concave faces are nearly identical to the P-face profiles of the corresponding T tubules. The ranges of particle densities measured on the microsomal concave faces are identical to the ranges measured on T-tubule cytoplasmic fracture faces. The mean particle densities of the microsomal concave fracture faces are similar to the average P-face densities of the respective T tubules as shown in Table I. These fracture faces are distinct from the concave fracture faces of microsomal SR which demonstrate much higher mean particle densities: $6,020/\mu m^2$ for normal and $5,470/\mu m^2$ for dystrophic muscle.

It can be seen from the profiles that the particle density ranges of the T system and the respective SL overlap, as indicated above the histograms in Figs. 4 and 5. In fact, the normal sarcolemmal E-

face particle density profile resembles the normal T-tubular P-face profile. Although one may confuse the particle density profiles of these two leaflets, and therefore confuse the identity of the microsomal fracture faces, the normal SL remains distinct by the presence of caveolae and by its P-face profile. There were no apparent structural manifestations of the caveolae observed among the microsomal fracture faces. If microsomes were derived from the SL, we would also expect to see a pronounced asymmetry in particle disposition between the microsomal concave and convex fracture faces that would reflect the much higher mean sarcolemmal P-face particle density ($1,630/\mu m^2$). Such high particle densities were never observed among the concave or convex fracture faces.

The results of the biochemical experiments further substantiate the stereological and other morphological evidence of T-tubule isolation. The lack of specific Na^+, K^+-ATPase activity observed for native and detergent-treated T-tubular membranes of normal and dystrophic muscle indicates that little contamination from the SL is present in these preparations. Furthermore, polyacrylamide gel electrophoresis of dystrophic T-tubular membrane proteins demonstrates the absence of high molecular weight proteins characteristic of sarcolemmal membranes (18). Moreover our T-tubular fraction is obtained without the use of harsh salt extractions (using LiBr or KI) and Polytron (Brinkmann Instruments, Inc., Westbury, N. Y.) sonication techniques commonly required to produce a microsomal fraction of sarcolemmal membranes. In the absence of sonication and with simple homogenization with a Waring blender (Waring Products Div., Dynamics Corp. of America, New Hartford, Conn.), sarcolemmal mem-

branes appear as membrane sheets and are found principally in the nuclear fraction (22). It therefore appears unlikely that our T-tubular preparations contain significant amounts of sarcolemmal membrane fragments.

Although the agreement is good between the microsomal and T-tubular fracture face profiles, there are some small differences. A redistribution of intercalated proteins during isolation of the microsomal subfraction is the most likely source of differences observed. Surfaces are exposed to the various incubation media that otherwise have no communication with the extracellular space *in situ*. Integral membrane proteins may be stabilized by surface interactions comparable to the role of spectrin in erythrocyte ghosts (9). Homogenization of the tissue and exposure to the solutions used in the isolation of the microsomes could presumably disrupt such surface interactions and alter the freeze-fracturing behavior of these membranes. The small differences in the particle distributions could be explained by a redistribution of integral proteins within the plane of the membrane either during isolation or during freezing as a consequence of destabilized surface interactions. Such particle movements were described recently during the isolation of secretory granules (21).

Another source of differences is membrane inversion during isolation. In the case of isolated rabbit SR, such inversion is easily detected in freeze-fracture replicas due to the high asymmetry of this membrane, but estimates of inversion are <3% in our laboratory (unpublished observation).

The similarities of the concave microsomal fracture face distributions and the cytoplasmic fracture face distributions from intact T tubules is strong evidence that the microsomes are derived from the transverse tubules. Furthermore, differences in the particle distributions between intact normal and dystrophic T tubules are also reflected in the corresponding microsomal concave fracture-face particle distributions.

Other attempts to isolate a purified fraction of T-tubular membrane have been described recently (1, 5, 6, 12, 13). However, these preparations appeared to contain a heterogeneous population of membrane types. Furthermore, little attempt to identify sarcolemmal contamination was presented. We believe that freeze fracturing provides a good measure of purity through a stereological analysis of the fracture faces. The absence of SR membranes in our preparation is clearly revealed by the stereological data. There were no concave

fracture faces with even the minimum particle density characteristic of SR. In addition, there was no evidence of inside-out SR vesicles that would produce high density convex fracture faces. Contaminating membranes may be present, however, because the sampling procedure eliminates small fracture faces or faces with cast shadows. However, none of the concave fracture faces eliminated for these reasons appeared to have a particle density high enough to be SR, and electrophoretic gel patterns did not demonstrate the protein pattern of SR. Contamination by the SL is difficult to rule out on stereological grounds, but the biochemical data suggest that this membrane is absent as well.

Structural and Functional Alterations in Dystrophic Sarcotubular Membranes

In a previous communication (19) we suggested that one of the early manifestations of the dystrophic process (i.e. before muscular atrophy occurs) is a proliferation of sarcotubular membranes in the junctional region (particularly the junctional SR and T tubules). The proliferation of junctional membranes has recently been quantified by stereological analysis of thin-sectioned dystrophic chicken muscle (4). The author showed that the dystrophic process is accompanied by an 88% increase in T-tubular volume density and a 62% increase in surface density. Similar proliferation of dystrophic junctional SR membranes was observed.

In this study, we demonstrate that the proliferation of dystrophic T-tubular membranes is accompanied by a significant reduction in mean particle density for both isolated and intact T-tubular membranes. A similar reduction in mean particle density is observed for freeze-fracture P faces of dystrophic SL and is in agreement with the findings of other investigators using human muscle tissue (20).

The morphological changes in the sarcotubular system in this and previous work are accompanied by a significant increase in the Ca^{2+}-ATPase activity of dystrophic T tubules (Table III) as well as an impairment of the calcium-transporting ability of dystrophic SR reported in previous communications (17, 19). These data indicate that all three membranes which mediate excitation-contraction coupling (i.e., the SL, T tubules, and SR) are altered by the dystrophic process and may be responsible for the observed abnormalities in contractile properties of dystrophic muscle. Further-

more, these alterations suggest that a general membrane defect may be involved in the etiology of avian muscular dystrophy.

CONCLUSION

It is possible to separate a light fraction of vesicles from heterogeneous microsomal preparations of skeletal muscle. This light fraction is homogeneous and appears to contain no membranes from the SR. Stereological analysis shows that these light microsomes originate from the transverse tubules and enclose the extracellular space, i.e., the concave fracture faces correspond to the cytoplasmic P faces of the T tubules. We have succeeded in isolating a pure subfraction of sealed vesicles of transverse tubular membrane. This membrane has been an elusive link in the scheme of excitation-contraction coupling, and with these methods it may be possible to explain alterations in the contractile behavior of dystrophic muscle.

REFERENCES

1. BARCHI, R. L., E. BONILLA, and M. WONG. 1977. Isolation and characterization of muscle membranes using surface-specific labels. *Proc. Natl. Acad. Sci. U. S. A.* **74**:34-38.
2. BASKIN, R. J. 1970. Ultrastructure and calcium transport in dystrophic chicken muscle microsomes. *Lab. Invest.* **23**:581-589.
3. BASKIN, R. J. 1974. Ultrastructure and calcium transport in microsomes from developing muscle. *J. Ultrastruct. Res.* **49**:348-371.
4. BERINGER. T. 1978. Stereologic analysis of normal and dystrophic avian αW myofibers. *Exp. Neurol.* **61**:380-394.
5. BLAISE-SMITH, P. B., and S. H. APPEL. 1977. Isolation and characterization of the surface membranes of fast and slow mammalian skeletal muscle. *Biochim. Biophys. Acta.* **466**:109-122.
6. CASWELL, A. H., Y. H. LAU, and J. P. BRUNSCHWIG. 1976. Ouabain-binding vesicles from skeletal muscle. *Arch. Biochem. Biophys.* **176**:417-430.
7. CROWE, T., and R. BASKIN. 1978. Freeze fracture of intact sarcotubular membrane. *J. Ultrastruct. Res.* **62**:147-154.
8. DEAMER, D. 1973. Isolation and characterization of a lysolecithin-adenosine triphosphatase complex from lobster muscle microsomes. *J. Biol. Chem.* **248**:5477-5485.
9. ELGSAETER, A., and D. BRANTON. 1974. Intramembrane particle aggregation in erythrocyte ghosts. I. The effects of protein removal. *J. Cell Biol.* **63**:1018-1030.
10. JORGENSEN, P. L., and J. C. SKOU. 1969. Preparation of lightly active (Na⁺ + K⁺)-ATPase from the outer medulla of rabbit kidney. *Biochem. Biophys. Res. Commun.* **37**:39-46.
11. LANGER, G. A., J. S. FRANK, and K. D. PHILIPSON. 1978. Preparation of sarcolemmal membrane from myocardial tissue culture monolayer by high-velocity gas dissection. *Science (Wash. D. C.)* **200**:1388-1391.
12. LAU, Y. H., A. H. CASWELL, and J.-P. BRUNSCHWIG. 1977. Isolation of transverse tubules by fractionation of triad junctions of skeletal muscle. *J. Biol. Chem.* **252**:5565-5574.
13. LAU, Y. H., A. H. CASWELL, J.-P. BRUNSCHWIG, R. J. BAERWALD, and M. GARCIA. 1979. Lipid analysis and freeze fracture studies on isolated transverse tubules and sarcoplasmic reticulum subfractions of skeletal muscle. *J. Biol. Chem.* **254**:540-546.
14. LAU, Y. H., A. H. CASWELL, M. GARCIA, and L. LETELLIER. 1979. Coupled sodium, potassium and chloride transport in isolated transverse-tubules of rabbit skeletal muscle. *Biophys. J.* **25**:27 a.
15. LOSA, G. A., E. R. WEIBEL, and R. P. BOLENDER. 1978. Integrated stereological and biochemical studies on hepatocytic membranes. III. Relative surface of endoplasmic reticulum membranes in microsomal fractions estimated on freeze-fracture preparations. *J. Cell Biol.* **78**:289-308.
16. MALOUF, N., and J. SOMMER. 1976. Chicken dystrophy: The geometry of the transverse tubules. *Am. J. Pathol.* **84**:299-316.
17. SABBADINI, R., D. SCALES, and G. INESI. 1975. Ca²⁺ transport and assembly of protein particles in sarcoplasmic membranes isolated from normal and dystrophic muscle. *FEBS (Fed. Eur. Biochem. Soc.). Lett.* **54**:8-12.
18. SABBADINI, R., D. SCALES, and C. NIXON. 1978. A novel technique for the isolation of transverse tubular membrane from dystrophic skeletal muscle. Proceedings of the Ninth International Congress on Electron Microscopy. J. Sturgess, editor. **2**:640-641.
19. SCALES, D, R. SABBADINI, and G. INESI. 1977. The involvement of sarcotubular membranes in genetic muscular dystrophy. *Biochim. Biophys. Acta.* **465**:535-549.
20. SCHOTLAND, D. L., E. BONILLA, and M. VAN METER. 1977. Duchenne dystrophy: alteration in muscle plasma membrane structure. *Science (Wash. D. C.)* **196**:1005-1007.
21. SCHULER, G. 1978. Particle clustering in secretory granule membranes induced by centrifugation: freeze-fracture analysis using different cryofixations. Proc. Ninth International Congress on Electron Microscopy. J. Sturgess. editor. **2**:150-151.
22. SEVERSON, D. L., G. I. DRUMMOND, and P. V. SULAKHE. 1972. Adenylate cyclase in skeletal muscle, Kinetic properties and hormonal stimulation. *J. Biol. Chem.* **247**:2949-2958.
23. WEIBEL, E. R., G. LOSA, and R. P. BOLENDER. 1976. Stereological method for estimating relative membrane surface area in freeze-fracture preparations of subcellular fractions. *J. Microsc. (Oxf.).* **107**:255-266.
24. YAP, J. L., and D. H. MACLENNAN. 1976. Characterization of the adenosinetriphosphatase and calsequestrin isolated from sarcoplasmic reticulum of normal and dystrophic chickens. *Can. J. Biochem.* **54**:670-673.